Integrated Approach to Studying the Development and Final Network Properties of Urethane Acrylate Coatings

Susan M. Gasper,* David N. Schissel,* Linda S. Baker, Diane L. Smith, Randall E. Youngman, Lung-Ming Wu, Susan M. Sonner, Robert R. Hancock, Carrie L. Hogue, and Steven R. Givens

Corning Incorporated, Corning, New York 14831

Received September 2, 2005; Revised Manuscript Received January 12, 2006

ABSTRACT: An integrated approach, involving the use of a number of analytical techniques, was used to study polymer coating network development during photopolymerization of a series of fast reacting, low modulus coating formulations containing urethane/acrylate oligomers and acrylic comonomers. Real-time UV rheology measurements, to assess the development of viscoelastic properties, and real-time FTIR, to assess the disappearance of acrylic groups, were used to study the early stages of the photocuring reaction up to the gel point. These results showed that the development of the cross-linked network and the rate at which acrylate double bonds reacted were not necessarily directly proportional as might be expected and were dependent upon the structures of the urethane/acrylate oligomer and comonomers comprising a particular coating. Samples of partially polymerized coatings were also prepared having degrees of acrylate conversion ranging from ∼50% through full conversion. Analysis of the amount of extractable material and the molecular weight distribution of soluble oligomeric material as a function of degree of conversion also showed a dependence upon the coating formulation components. In some cases the extraction results for intermediate cure level samples could be correlated to the reactivity trends observed in the early stages of the curing reaction. We also made use of solid-state NMR ^{1}H T_2 relaxation measurements to assess both partially and fully reacted films. The rate of magnetization decay correlated well with both the developing level of cross-link density as the degree of polymerization increased and also with the theoretical cross-link densities expected for the fully cured networks based on the structure of the coating formulation components. The latter also correlated well with modulus measurements made on fully cured coating film samples.

Introduction

Photopolymerization of acrylic materials to prepare cross-linked coatings for a variety of applications is widespread.[1] The versatility of these materials originates in the ability of light to transform a solvent-free, liquid mixture into a solid almost instantaneously, with a range of properties available through the judicious choice of coating components. This ease of preparation and versatility of properties have made them ideal materials for use in a wide variety of applications, including inks, adhesives, packaging materials, and protective coatings for optical fibers. While this transformation from liquid to solid appears to be straightforward, a complex interplay between chemical reactions and physical restraints is taking place during the photopolymerization process. The resulting polymer network topology and eventual cured coating performance properties are governed by this interplay, which is often neglected until performance issues arise. A fundamental understanding of the photocuring process is needed in order to avoid or minimize such issues. This understanding would also facilitate some degree of control over the relationship between the chemical structure of liquid coating components, network structure of the cross-linked polymer, and mechanical and other properties in these high-performance coatings in a particular application. For example, in the case of optical fiber, properties such as fiber durability and optical signal strength are highly dependent upon the properties of the coating materials.

A number of approaches have been taken to study both final network structure and network development in photoinitiated polymerizations. Many of these have been aimed at relating the chemical changes that take place during the polymerization reaction to the development of mechanical properties in fully reacted materials. Use has been made of both static and dynamic measurement techniques. Static measurements have most often focused on the characterization of fully polymerized materials, but they have also been applied to samples that have been reacted to an intermediate level. Dynamic, real-time measurements have been used to continuously monitor both how various chemical and physical properties change during the polymerization process as well as the rates at which they are changing.

Most commonly, the progress of photopolymerization reactions of acrylic materials has been followed by monitoring the disappearance of the reactive acrylic groups present in monomers and oligomers. Real-time FTIR, as pioneered by Decker and co-workers,[2] has emerged as one of the most useful techniques for this purpose. Real-time UV[3] and NMR[4,5] have also been applied to these systems. NMR has also been used to study fully polymerized systems in order to characterize the types of structural linkages present as a result of cross-linking reactions or chain transfer processes that occur during the reaction.[6] The progress of these reactions has also been studied by monitoring the heat of polymerization evolved using photo-DSC.[7] In addition to the techniques that focus on the disappearance of particular reactive groups, extraction experiments have been used to monitor residual, unreacted acrylic materials that have not been incorporated into the developing polymer network. While most of these studies have focused on the extraction of material remaining after the system has reached its highest conversion level, some extraction studies have been done on systems at intermediate conversion levels to gain some

* To whom correspondence is to be addressed: gaspersm@corning.com, schisseldn@corning.com.

10.1021/ma051918j CCC: $33.50
Published on Web 02/14/2006

insight into how individual coating components incorporate into the developing polymer network.[8]

Photo-cross-linked systems have also been studied using methods that focus on the measurement of properties related to the development of cross-link density as the polymerization reaction proceeds. Commonly, dynamic mechanical analysis and Instron testing of stress−strain properties are done on fully polymerized systems.[1] Rheological monitoring of the development of viscoelastic properties in real time has been used to determine the point at which gelation occurs in photo-cross-linked systems.[9,10] Solid-state NMR relaxation measurements, in which the rate of ^{1}H bulk magnetization decay is related to the extent of cross-link density, have provided useful information regarding the network structure of polymeric materials.[11,12] These NMR techniques, as well as the transfer of magnetization between ^{1}H and ^{13}C,[13] or the magnetic relaxation[14] of individual groups of atoms (i.e., ^{13}C NMR resonances from specific functional groups), have all been utilized to gain insights into the nature of the cross-linked polymer network, including network defects. Other NMR approaches have included the use of isotopic labeling to enable ^{2}H wide-line NMR and related relaxation measurements.[15] In addition, fluorescence techniques, in which the intensity of fluorescence in a probe molecule that is either dispersed in or chemically attached to a cross-linked polymeric network provides information on the molecular environment, have also been used to study the network structure of photopolymerized materials.[4,16,17]

While the published studies on acrylate photopolymerizations using these different analytical approaches have provided many valuable insights into these systems, such as the observation that the buildup of modulus in the cross-linked network does not necessarily linearly relate to the chemical conversion of acrylate groups,[10] many of the studies have been limited to very simple systems. Usually coatings consisting of a single difunctional material, or a difunctional material and one monofunctional comonomer, along with a single photoinitiator are studied. Also, very few photopolymerization studies employing UV curable urethane/acrylate oligomers, which are often used in performance coatings because of the wide range of desirable properties they can introduce, have been reported.[18] In addition, many of the published studies focus on slower polymerizing methacrylate systems rather than the more reactive acrylates. Consequently, the link between most of these systems and actual extremely fast polymerizing, high-performance coatings (containing oligomeric components, additional monomers and additives—such as optical fiber coatings) has been somewhat limited.

To address this gap, we have investigated polymer network development during photocuring in a series of model coatings more closely related to those of the very low modulus urethane/acrylate coatings we have an interest in.[19] These coatings are very fast polymerizing mixtures of high molecular weight urethane/acrylate oligomers and different acrylic comonomers. In the work reported here we have taken an integrated approach to the study of these coatings systems, making use of different analytical methods to study the fully cured polymer network as well as the developing network during various stages of partial curing. By combining kinetic measurements, such as real-time FTIR and UV rheology, with extraction studies to monitor the incorporation of reactive materials into the network at various curing levels, and also making use of NMR relaxation measurements,[20] along with dynamic mechanical analysis and Instron testing of fully polymerized networks, we have attempted to develop a more comprehensive picture of network development as a function of component structure in these coatings. This knowledge can then be used to design new coatings with specific performance properties or in the analysis and understanding of performance issues related to coating defects.

Experimental Section

Materials. The poly(propylene glycol) materials (PPG2000 and PPG8000) were purchased from Bayer (Acclaim 2200 and Acclaim 8200), as was the Desmodur W (4,4′-methylenebis(cyclohexyl isocyanate), H12MDI). The 2-hydroxyethyl acrylate (HEA), dibutyltin dilaurate, and 2,6-di-*tert*-butyl-4-methylphenol (BHT) were purchased from Aldrich Chemical Co. The Photomer 4003 (ethoxylated (4) nonylphenol acrylate) and Photomer 8061 (propoxylated (3) methyl ether acrylate) were from Cognis. Irgacure 184 and 819 were from Ciba Specialty Chemicals. The polyols were heated at 40−50 °C for 12 h under vacuum to remove traces of water prior to use. All of the other materials were used as received.

Oligomer Preparation. The oligomers were prepared from poly(propylene glycol), 4,4′-methylenebis(cyclohexyl isocyanate), and hydroxyethyl acrylate using well-known procedures.[21−24] The first oligomer was prepared from 1 mol of $M_n = 2000$ poly(propylene glycol), 2 mol of the diisocyanate, and 2 mol of the hydroxyethyl acrylate and is designated 1xPPG2000. The second oligomer was prepared in a similar fashion using $M_n = 8000$ poly(propylene glycol) and is designated 1xPPG8000. The third oligomer was prepared from 2 mol of $M_n = 2000$ poly(propylene glycol), 3 mol of diisocyanate, and 2 mol of hydroxyethyl acrylate and is designated 2xPPG2000.

Formulation Preparation. The oligomer and comonomers were hand-mixed at 55 °C until thoroughly blended. Then the photoinitiator was mixed in until most of it had dissolved. The mixture was heated overnight in a 50−55 °C oven and then mixed again. All of the coatings prepared appeared to be uniformly mixed. Compositions were verified using HPLC and GPC. Viscosity measurements were obtained using a Brookfield CAP 2000L viscometer at 25 °C with a no. 4 spindle cone used at 50 rpm.

Film Preparation and Photopolymerization Procedures. Wet films were cast on silicone release paper with the aid of a drawdown box having a 5 mil gap thickness. Fully polymerized films were prepared using a Fusion Systems UV curing apparatus with a 600 W/in. D-bulb (50% power, 10 ft/min belt speed, nitrogen purge). Polymerized film thickness was between 3 and 4 mil. Partially polymerized films were prepared using a Fusion Systems UV curing apparatus with a 300 W/in. D-bulb on a high-speed, unpurged cure belt. Wet films cast on release paper were placed in a box with a fused silica window and purged for 2 min with nitrogen at a flow rate of 10 mL/min. An aluminum plate with a narrow slit was placed beneath the face of the lamp in order to cut the light intensity. Radiation dose was further controlled using standard laboratory tissue as a neutral density filter. Belt speed and neutral density filter thickness were adjusted to give the desired conversion level. Degrees of conversion were determined on a Bruker Vector FTIR spectrometer by monitoring the acrylate bond (1406 cm^{-1}). Average conversion values were calculated from degrees of conversion determined for the top and bottom sides of the film at three locations along the length. The dose received by the films in the cure box was measured with an IL390 light bug.

Real-Time FTIR. The rate of conversion of acrylate bonds (1406 cm^{-1}) upon exposure to UV−vis radiation was monitored by FTIR on a Bruker IFS 66S spectrometer. Films with 1 mil thickness were drawn directly on a 3 bounce diamond-coated ZnSe crystal in an ASI DuraSamplIR accessory and purged with nitrogen for 1 min. Mid-infrared spectra from 4000 to 650 cm^{-1} were collected at 6 ms intervals for 0.9 s prior to UV exposure. UV irradiance from a Lesco Mark II spot cure unit conducted through a liquid light guide measured ∼15−20 mW in the UVA region (320−390 nm). The reaction was monitored for 5 s after a relatively short initial light pulse, and then the sample was exposed to a longer pulse to

Table 1. Summary of Formulations Studied

sample	formulation (oligomer/comonomer)	calculated g/mol of x-linking acrylate	initial viscosity (P) at 25 °C)
O1	16 1xPPG2000//81 Ph4003	8460	6.3
O2	52 1xPPG2000//45 Ph4003	2650	56
O3	52 1xPPG8000//45 Ph4003	8420	151
M1	52 2xPPG2000//45 Ph4003	4830	90
M2	52 2xPPG2000//45 Ph8061	4830	17
M3	52 2xPPG2000//22.5 Ph4003/22.5 Ph8061	4830	34

achieve maximum conversion. Degrees of conversion were calculated independently for each spectrum collected and plotted on a time scale. Composite conversion rate values were assigned as the slope of the linear portion of the conversion vs time curve (10−40%).

UV Rheology. A Rheometric dynamic rheometer, RDA-II, was modified such that the sample between parallel plates could be exposed to UV while its viscoelastic property was measured in real time. A UV source (Green Spot) and a precision shutter system (Uniblitz VMM-T1) were used. The UV output was monitored with a hand-held radiometer (EIT SpotCure) located at the end of the light guide, with consistent readings of ~3 W/cm^2. The UV intensity measured at the sample surface was 16 mW/cm^2.

Electric signals, corresponding to rotational position and torque, were collected and processed to give fundamental parameters of viscoelasticity, i.e., dynamic shear modulus, viscous modulus, elastic modulus, and damping factor (tan δ). An experiment begins with loading of the liquid between the parallel plates with a gap setting of 0.025 mm. The rheometer begins to oscillate at 10 Hz with a 30% strain amplitude, as the responding torque is monitored. The UV is turned on for a total of 4 s, while all formulations gel well within 2 s. At about 10 s, the UV is turned on again for an additional 40 s to "completely" polymerize the coating. Because the experiment is run at a single frequency, we are not able to determine the gel point according to the Winter-Chambon criterion,[25] but rather use the alternative definition of the attainment of a 45° phase angle (tan $\delta = 1$) as the damping factor decreases as an indicator of the critical gel point.[26]

Ultrasonic Extraction Procedure. Polymerized films were extracted three times, for 30 min, using methylene chloride and an ultrasonic extraction technique. Lower molecular weight components recovered in the extracts were characterized by reversed phase HPLC using a C18 column (Intersil ODS-2 5 μm or ODS-3 3 μm, 150 mm × 4.6 mm Alltech Associates), 40 °C, acetonitrile−water gradient elution, and photodiode array detection (220 nm). The oligomeric components were characterized by GPC using tetrahydrofuran and two mixed D columns followed by one 100 Å column all 5 μm × 300 mm (Polymer Laboratories Ltd.) at 40 °C with refractive index detection. External standards were used for quantification of components while polystyrene standards were used to evaluate molecular weight distributions (Polymer Laboratories Easi-Cal PS-2 A and B standards plus PS-980 and PS-162).

NMR Measurements. ^{1}H NMR data were collected using a commercial instrument and probes (Chemagnetics), in conjunction with a 4.7 T superconducting magnet. At this field strength, the resonance frequency for ^{1}H is 199.8 MHz. ^{1}H T_2 relaxation measurements were conducted using a Hahn echo pulse sequence to monitor the signal strength as a function of delay time between the $\pi/2$ and π pulses. The pulse widths were typically 2.3 and 4.6 μs, respectively. All measurements in this study were made with solvent swelling at room temperature. Samples were loaded into short 5 mm glass NMR tubes in which a small quantity of glass wool was added to keep the samples submerged in solvent. Approximately 0.2 mL of deuterated methylene chloride (CD_2Cl_2) was added immediately before data acquisition. Subsequent measurements after the samples had been swollen in solvent for longer times, up to 1 day, showed that swelling in CD_2Cl_2 was very efficient and that these data did not change as a function of time in solvent. The ratio of solvent to sample was also evaluated, as this parameter has been shown to influence the ^{1}H T_2 relaxation times,[27] but it was determined that all samples were studied using excess solvent and that the solvent/sample ratio was not a factor in these particular measurements.

The ^{1}H Hahn echo data were evaluated by taking the height of the time domain echo in magnitude mode and subsequently plotting the normalized values as a function of delay time. In this manner, ^{1}H decay curves were generated using the bulk proton signal from each sample and therefore these data represent the characteristic properties of the entire sample. We did not attempt to process the NMR data and obtain similar curves for distinct ^{1}H NMR resonances. Numerical analysis of the ^{1}H decay curves was performed using the model of Kuhn et al.,[28] mathematically described by the relation

$$M(t) = A\exp\left\{\left(-\frac{t}{T_2}\right)-\left(\frac{qM_2t^2}{2}\right)\right\} + B\exp\left(-\frac{t}{T_2}\right) + C\exp\left(-\frac{t}{T_2^{sol}}\right) \quad (1)$$

where the prefactors *A*, *B*, and *C* denote the fractional contributions from material having three distinct degrees of mobility, roughly corresponding to fully cross-linked chains, dangling chain ends, and sol components, respectively. This description also provides information on two time constants, T_2 and T_2^{sol}, which are related to the incorporated and unincorporated material in these polymeric films. Finally, the qM_2 parameter describes the anisotropic motion of the dangling chain ends and has been used to evaluate cross-link density in other types of polymers.[29,30] This model is very similar to a variety of other models, although many of these involve additional parameters to describe correlation times[31,32] or treat the anistropic motion of the dangling ends in a different manner (BPP-type T_2 relaxation).[33] Several recent studies have shown that the choice of models for fitting bulk ^{1}H T_2 relaxation curves from rubbery materials can be fairly ambiguous[34] as well as inadequate.[35] We have chosen the above relation due to its relative simplicity (fewer fitting parameters) and use it to quantify the various fractions of cross-linked, dangling ends, and sol components in our polyurethane acrylate materials. We also obtain the two T_2 time constants and a value for qM_2. However, the qM_2 values obtained from such treatment of our data are not further evaluated at this time, as this is beyond the scope of the current study. All fits to the ^{1}H T_2 decay curves were obtained using commercial software.

Mechanical Testing Procedures. Fully polymerized films were allowed to age (23 °C, 50% rh) for at least 16 h prior to testing. Film samples were cut to a specified length and width (15 cm × 1.3 cm). Young's modulus, tensile strength at break, and elongation at break were measured using an Instron 5500 tensile tester. Films were tested at an elongation rate of 2.5 cm/min starting from an initial jaw separation of 5.1 cm. Glass transition temperatures of the fully polymerized films were determined by the tan δ curves measured on a Seiko-5600 DMS in tension at a frequency of 1 Hz.

Results and Discussion

Two series of model coating formulations were studied in this work. These are summarized in Table 1, and structures of the oligomers and monomers used are shown in Table 2. In the first series, designated O1 to O3 and which will subsequently be referred to as the O series, two urethane/acrylate oligomers (designated as 1xPPG2000 and 1xPPG8000 to indicate that the oligomers had single poly(propylene glycol) blocks of 2000 and

Table 2. Structures of Oligomers and Comonomers

Material	Structure
1xPPG$_x$	HEA~H12MDI~PPG$_x$~H12MDI~HEA
2xPPG$_x$	HEA~H12MDI~PPG$_x$~H12MDI~PPG$_x$~H12MDI~HEA
Photomer 4003	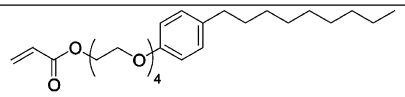
Photomer 8061	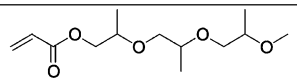

8000 molecular weight) were formulated at different oligomer/monomer weight ratios with the same comonomer, Photomer 4003 (ethoxylated nonylphenol acrylate), to give coatings expected to have different cross-linking levels when fully reacted. The O3 formulation (1xPPG8000) had the same oligomer/monomer weight ratio as the O2 (1xPPG2000) formulation, but with a different cross-link level. The O1 formulation (1xPPG2000) had the same expected cross-link level as O3, but with a different oligomer/monomer weight ratio. In the second series, designated M1 to M3 and subsequently referred to as the M series, the oligomer 2xPPG2000 (oligomer having two poly(propylene glycol) blocks of molecular weight 2000) was formulated with different comonomers at a 52/45 oligomer/monomer weight ratio to give coatings which should have similar cross-linking levels. In this series both Photomer 4003 and Photomer 8061 (propylene glycol monomethyl ether acrylate) were used as comonomers, either individually or as a 50/50 mixture. In both sets of formulations the total photoinitiator level was set at 3 wt %, consisting of equal parts Irgacure 184 and Irgacure 819.

The nature of the oligomer synthesis, as well as the polydisperse nature of the polyol reactants, ensures that the oligomers would consist of a mixture of materials having a distribution of molecular weight values.[36,37] Throughout our discussion we make the assumption that the various oligomers have a molecular weight equal to that of the ideal structure based on reactant stoichiometry described in the Experimental Section (and as shown in Table 2). GPC measurements (data not shown) did confirm that the various oligomers had average molecular weights (relative to poly(styrene) standards) in the correct order (i.e., 1xPPG2000 < 2xPPG2000 < 1xPPG8000). Idealized cross-linking levels (in grams of material per mole of cross-link) were calculated by assuming that the only cross-linking points were the acrylic end groups on the oligomers. The cross-linking levels are therefore determined by the amount and molecular weight of oligomer in a given formulation. The calculated cross-link density levels are also shown in Table 1.

Because the materials examined in this study were extremely fast curing, we found it convenient to separate our study of the reaction into two parts. Kinetic measurement techniques were applied to the early stages of the curing reaction (0−40% conversion), roughly corresponding to reaction up to the gel point as determined by rheological measurements. Physical techniques to assess the structure of the developing polymer networks were applied at later stages of the reaction, from roughly 50% up to full conversion. The techniques included analysis of extracts from both partially and fully converted material, solid-state NMR relaxation studies on partially and fully polymerized networks, and dynamic mechanical analysis and stress−strain property testing on fully polymerized materials. The lightly cross-linked nature of the materials, as well as their rapid curing rates, made it difficult to directly obtain and analyze samples with a degree of conversion less than 50%.

Table 3. Early Stage Reaction Kinetic Data

sample	relative conv rate	gel time, t_{gel} (s)	DOC[a] at t_{gel} (%)
M1	65.48 ± 0.56	0.43 ± 0.02	26 ± 1
M2	40.48 ± 0.18	0.34 ± 0.05	14 ± 2
M3	51.23 ± 0.35	0.39 ± 0.04	20 ± 2
O1	69.19 ± 0.57	0.35 ± 0.01	22 ± 1
O2	82.37 ± 0.98	0.34 ± 0.01	21 ± 3
O3	61.43 ± 0.60	0.57 ± 0.04	30 ± 1

[a] Degree of conversion.

The kinetic data obtained for the early stages of the curing reactions are shown in Table 3 for both the O and M series of formulations. The relative conversion rates correspond to the slope in the time vs acrylate concentration plot in the 10−40% conversion range as explained in the Experimental Section. The gel time values were determined at the point at which storage and loss moduli became equal in the developing polymer network, and are expected to approximate the point at which a true, continuous load bearing network has been established.[11] Also included in the table are the approximate degree of conversion values at the gel point. These were determined from separate FTIR and UV rheology experiments using the same sample thickness and radiation dose.

For the M series of formulations, in which the same oligomer (2xPPG2000) and the same oligomer-to-monomer ratio (52/45) were used, the relative conversion rate increased as the rate of physical property development decreased (as indicated by an increase in t_{gel}). The fact that acrylate conversion is fast for M1 but network buildup is slow suggests that both reactive end groups of the cross-linking oligomer are not being incorporated efficiently at the early stages of the polymerization. For the M2 formulation, acrylate conversion is slow, but network buildup appears to be very efficient as indicated by the short t_{gel}. This would suggest that in M2 both reactive end groups of the cross-linking oligomer are being incorporated efficiently in the early stages of the polymerization. The low initial viscosity of M2 (Table 1) may allow the large growing polymer chain radicals to remain more mobile in the early stages of the reaction, which in turn allows them to more readily couple and form a cross-linked network. M1 has a higher initial viscosity, which could result in earlier diffusion-limited termination.[38] This would increase the rate of acrylate conversion (autoacceleration) but reduce the rate of large polymer chain radical coupling, resulting in an increase in t_{gel}.

The delayed gel point for M1 indicates that incorporation of both reactive end groups of the cross-linking oligomer is inefficient and suggests that the rapid acrylate conversion observed in this formulation must be dominated by the polymerization of the comonomer. The comonomer in M1 (Photomer 4003) differs from both the comonomer in M2 (Photomer 8061) and the 2xPPG2000 oligomer in that it has a hydrophobic alkylphenyl chain in addition to a rather hydrophilic polyether segment. In light of the amphiphilic, surfactant-like structure of Photomer 4003, one potential explanation for the fast acrylate conversion but slow network formation in M1 could be a greater tendency of the comonomer to self-associate and segregate itself from the oligomer. Surfactant-like association of Photomer 4003 to minimize interaction of hydrophobic alkylphenyl chains with the more hydrophilic polyether chains, both in the Photomer 4003 itself and in the oligomer, would increase the local concentration of acrylate groups associated with the comonomer,

Table 4. Formulation Acrylate Concentrations

formulation	relative[a] $[acrylate]_{total}$ (mol/g)	relative[a] $[acrylate]_{x-link}$ (mol/g)	relative[a] $[acrylate]_{monomer}$ (mol/g)
M1	1.08	0.18	0.89
M2	1.73	0.18	1.54
M3	1.40	0.18	1.22
O1	1.71	0.10	1.61
O2	1.23	0.34	0.89
O3	1.00	0.11	0.89

[a] Normalized to the total acrylate concentration in the O3 formulation.

thus leading to an increase in their polymerization rate. Enhanced polymerization rates attributed to hydrogen bonding which brings reactive acrylate groups into proximity have been suggested in other photocured systems.[39] The greater tendency of the Photomer 4003 acrylate groups to react with each other in the early stages of photopolymerization in the M series, in preference to the acrylate end groups in the oligomer which would build up the cross-linked gel network, results in delayed gelation. The measured conversion rates reflect the amount of Photomer 4003 in the formulations, decreasing in the order M1 (all Photomer 4003) > M3 (mix of the two monomers) > M2 (all Photomer 8061). The trend in both t_{gel} values and degree of conversion measured at the gel point (M1 > M3 > M2) reflects delayed gelation with increasing amounts of Photomer 4003. Because the fast conversion of the Photomer 4003 dominates the early stages of the reaction, the total molar amount of acrylate present in each formulation as well as the molar amount of acrylate coming from monomer (shown in Table 4), which both follow the order M2 > M3 > M1, does not appear to be important in this series.

For the O series formulations, the rate of acrylate conversion and the development of physical properties show a more direct relationship. The trend in the rate of acrylate conversion (O2 > O1 > O3) appears to be influenced by both initial viscosity and acrylate concentration. Although O1 has the highest level of acrylate, the rate of acrylate conversion is higher for O2, while the development of physical properties (indicated by t_{gel}) is nearly identical for the two formulations. The exceptionally low initial viscosity of O1 may delay the onset of autoacceleration relative to O2, leading to a lower overall acrylate conversion rate in the former. However, the initial low viscosity of O1 seems to facilitate the efficient incorporation of cross-linking oligomer into the network as suggested by t_{gel} and the degree of conversion at t_{gel} being equivalent to that for O2, despite a lower level of cross-linking acrylate in O1. In O2, a desirable balance of acrylate concentration and initial viscosity has been achieved to give a fast curing formulation. While the O3 formulation has the highest initial viscosity, it also has the lowest level of total acrylate concentration. The latter appears to control curing behavior in this formulation, as it exhibits the slowest conversion rate, the longest t_{gel}, and the highest conversion level at t_{gel}.

Another useful comparison is between O2, M1, and O3. These formulations have the same oligomer/monomer weight ratio and the same comonomer (Photomer 4003), and the molecular weight of the oligomer increases going from O2 (1xPPG2000) to M1 (2xPPG2000) to O3 (1xPPG8000). In this series the observed trends in both conversion rate (O2 > M1 > O3) and t_{gel} and degree of conversion at t_{gel} (O2 < M1 < O3) appear to be controlled more by acrylate concentrations than by the initial formulation viscosity. These trends are in fact opposite to what would be expected if increased initial coating formulation viscosity (O3 > M1 > O2) were to result in an earlier

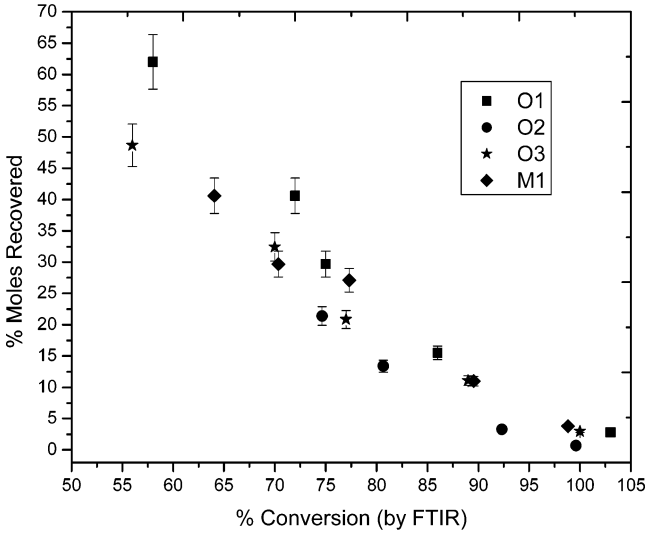

Figure 1. Photomer 4003 monomer recovery from O series and M1 film extracts.

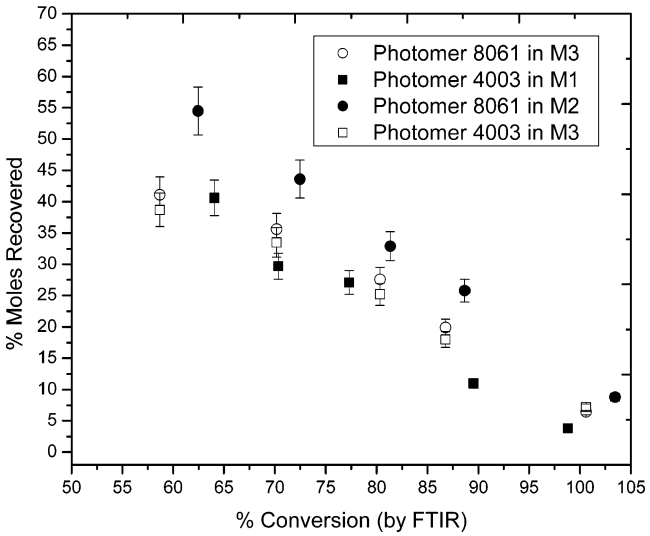

Figure 2. Monomer recovery from M series film extracts.

onset of autoacceleration. Increased acrylate conversion rate, shorter t_{gel}, and a lower degree of conversion at t_{gel} are seen in coatings having both the larger total acrylate concentration and the greater concentration of cross-linking acrylate groups from oligomer, indicating the more dominant role played by these factors.

The second set of experiments, involving analysis of extracts from partially polymerized coatings and solid-state NMR relaxation measurements on the partially developed polymer networks, were done on samples with a degree of conversion ranging from ~50% to full conversion. The molar percentage of monomer recovered from the various formulations as a function of degree of conversion is shown in Figures 1 and 2. The uncertainty in these measurements was estimated to be 7% based upon quantitation of a coating component believed not to change significantly during the curing process (data not shown) as well as a repeat series of extractions done on the M2 formulation. Although measurements of recovered, soluble oligomeric material were also made, shifts in the molecular weight distribution in this material in some samples compared to the starting oligomer introduced uncertainties into the quantitation. As a result, conclusions were not drawn using these data.

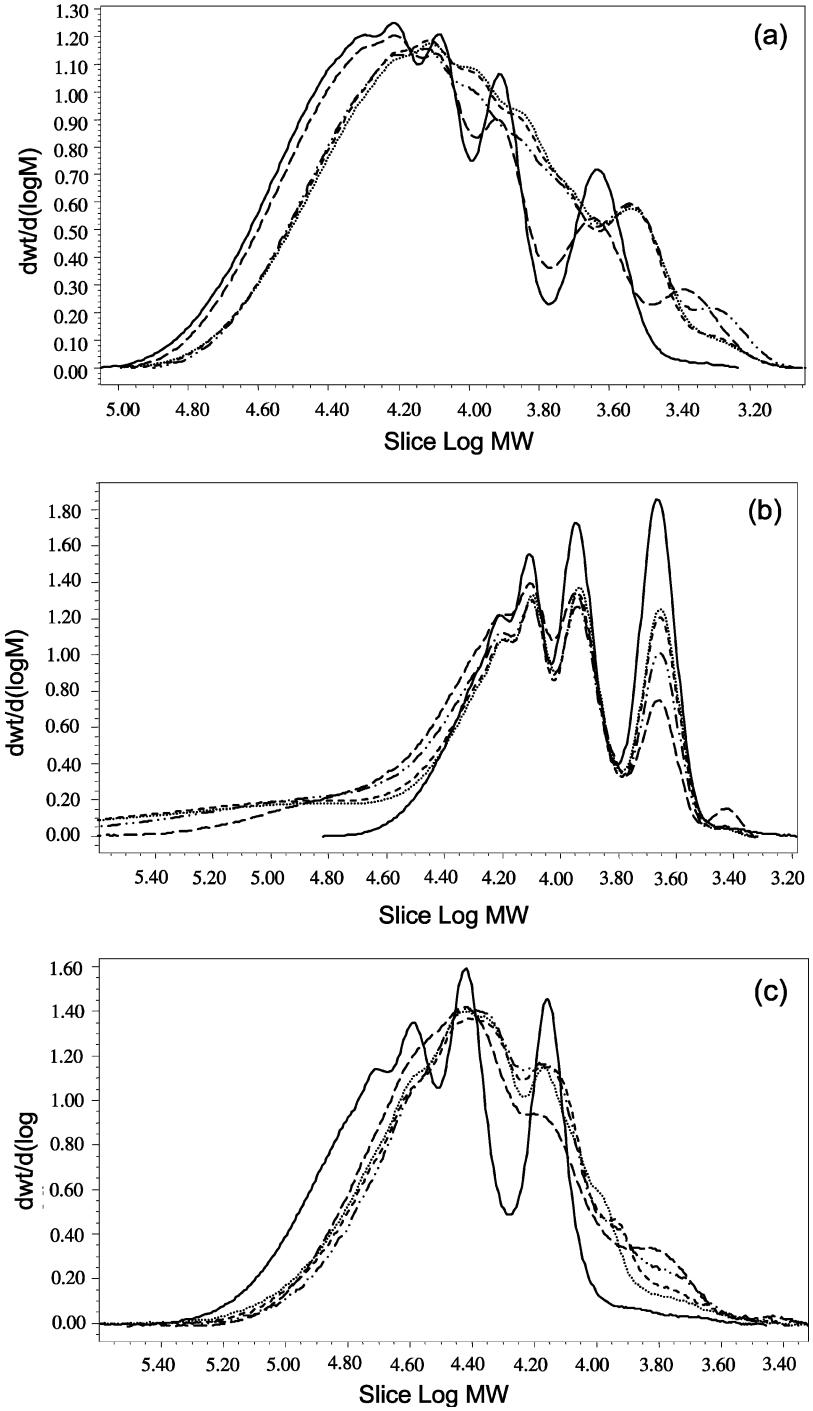

Figure 3. GPC molecular weight distribution profiles of M2 (a), O1 (b), and O3 (c) formulation extracts: (—) oligomer standard; (· · ·) extract from 60% cured film; (- - -) extract from 70% cured film; (— · ·) extract from 80% cured film; (— —) extract from 90% cured film.

With the exception of the O1 formulation at intermediate conversion levels, the molar amount of recovered Photomer 4003 at various conversion levels does not vary much for those samples in which it is the only comonomer (Figure 1). While the amount of Photomer 4003 recovered from O1 at intermediate conversion levels is slightly higher than in the other samples, as curing proceeds the O1 recovery levels of Photomer 4003 become similar to those observed in the other samples. The exceptionally high level of monomer in O1 compared to the other samples may account for this observation. While the recovery of Photomer 4003 from O2 is similar to the other samples at higher conversion levels, it was not possible to obtain data for conversion levels less than 70% in O2 for comparisons at these more intermediate levels of conversion.

Gel permeation chromatography (GPC) was also used to evaluate molecular weight distributions (MWD) of the soluble, recovered oligomeric material for the various partially polymerized samples. Unreacted monomer does not contribute to these distributions, as it is outside of the molecular weight range being monitored. The shift of MWD of recovered material to higher values for all conversion levels in the O1 sample (Figure 3b) suggests the formation of soluble, high molecular weight material from Photomer 4003 homopolymerization or the formation of material comprised of Photomer 4003 homopolymer fragments that have bonded to a urethane/acrylate oligomer before attachment to the growing, cross-linked network can take place. The data do not allow us to distinguish between the two possibilities. The formation of this type of unbound material

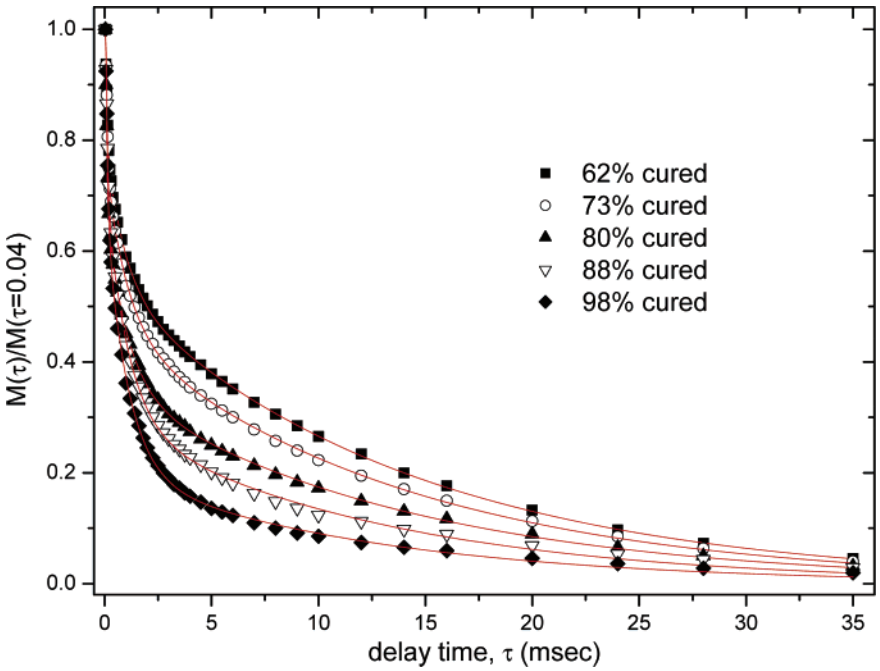

Figure 4. ^{1}H T_2 of partially cured solvent swollen M1 films. Symbols correspond to different acrylate conversion levels as determined by FTIR. Solid lines represent fitting of data using the modified Kuhn expression described in the text.

would be consistent with the suggestion that segregation of the Photomer 4003 molecules could be taking place to account for conversion rate differences and would be more likely to take place in the O1 coating in which the amount of monomer relative to oligomer is so much greater than in the other formulations. Recovery of the unbound, higher molecular weight material would also suggest less complete network formation in O1 compared to the other formulations. The poor quality of the O1 films, which were observed to easily fall apart and crumble into many small pieces during the extraction studies, is consistent with this. While little change was seen in the MWD of recovered material for the O2 sample (not shown), it was shifted to lower values for all conversion levels of O3 (Figure 3c). This indicates the formation of low molecular weight oligomeric Photomer 4003 homopolymer. Again this is consistent with self-association of the Photomer 4003 monomer, although in O3 the presence of much less monomer compared to oligomer than in O1 seems to limit the size of homopolymer chains formed.

In the M series, a slightly higher amount of the Photomer 8061 was recovered at all conversion levels in the M2 sample (where it is the sole comonomer) compared to either monomer in the M1 or M3 samples (Figure 2). This is consistent with the low conversion rate seen for M2. The Photomer 8061 and Photomer 4003 are consumed at similar rates when they are coreactants in the M3 sample. The proposed self association of Photomer 4003 would occur in both M1 and M3, and the compatibility of the two comonomers may be such that the Photomer 8061 participates in this segregation and reacts at a similar rate. In M2 a shift of recovered oligomer MWD to lower values is also seen at all conversion levels (Figure 3a). The MWD of recovered oligomer resembled starting material for both M1 and M3 (not shown). The unbound, oligomeric Photomer 8061 homopolymer that is extracted in M2 may be a consequence of slow monomer conversion rate coupled with a faster oligomer conversion rate—as indicated by the fairly short gel time resulting from a preference for difunctional oligomer reaction and network buildup in the early stages of the reaction. With oligomer tending to be depleted earlier, we might expect to see more oligomeric Photomer 8061 homopolymer in the 50−80% conversion range which has not had an opportunity to bind to the developing polymer network. For M1, we do not see unbound oligomeric Photomer 4003 homopolymer in this conversion range. At this point the Photomer 4003 homopolymer that is formed in the early part of the reaction as a result of the monomer segregation that was proposed to account for the fast conversion rate has had a chance to become bound into the cross-linked polymer network—presumably via chain transfer reactions. In contrast to M2, the gel time in M1 is greater because of the preference for monomer homopolymerization over oligomer reaction to build up the network in the early stages of the curing process.

The samples at intermediate conversion levels that were studied by extraction were also examined using solid-state NMR ^{1}H T_2 relaxation measurements. The data in Figure 4 show a signal decay curve for one representative model film (M1) as a function of conversion level. Decay curves for the other samples had a similar qualitative appearance. As one increases the level of conversion in these systems, the ^{1}H NMR signal for the bulk polymer appears to decay at a faster rate, as evidenced by the steeper decay curves for samples with higher conversion levels. The simple qualitative analyses of these types of data demonstrate that such NMR measurements are very sensitive to differences in degree of conversion and can be useful in following the network development of polyurethane acrylate films. Similar measurements were also made on all M and O series samples, and in almost all instances the films with lower conversion level have a shallower decay when the Hahn echo magnitude is plotted against echo decay time. As the film polymerizes and cross-linking increases, the ^{1}H T_2 curves become steeper.

The modified Kuhn formalism[28,40] allows us to adequately fit these ^{1}H T_2 data, as shown by the curves in Figure 4. This model contains two relaxation time constants as well as prefactors related to the relative populations of the following: fully cross-linked chains, dangling chain ends, and sol (unincorporated) material. These terms, which reflect the original modified Kuhn treatment terminology, may be somewhat

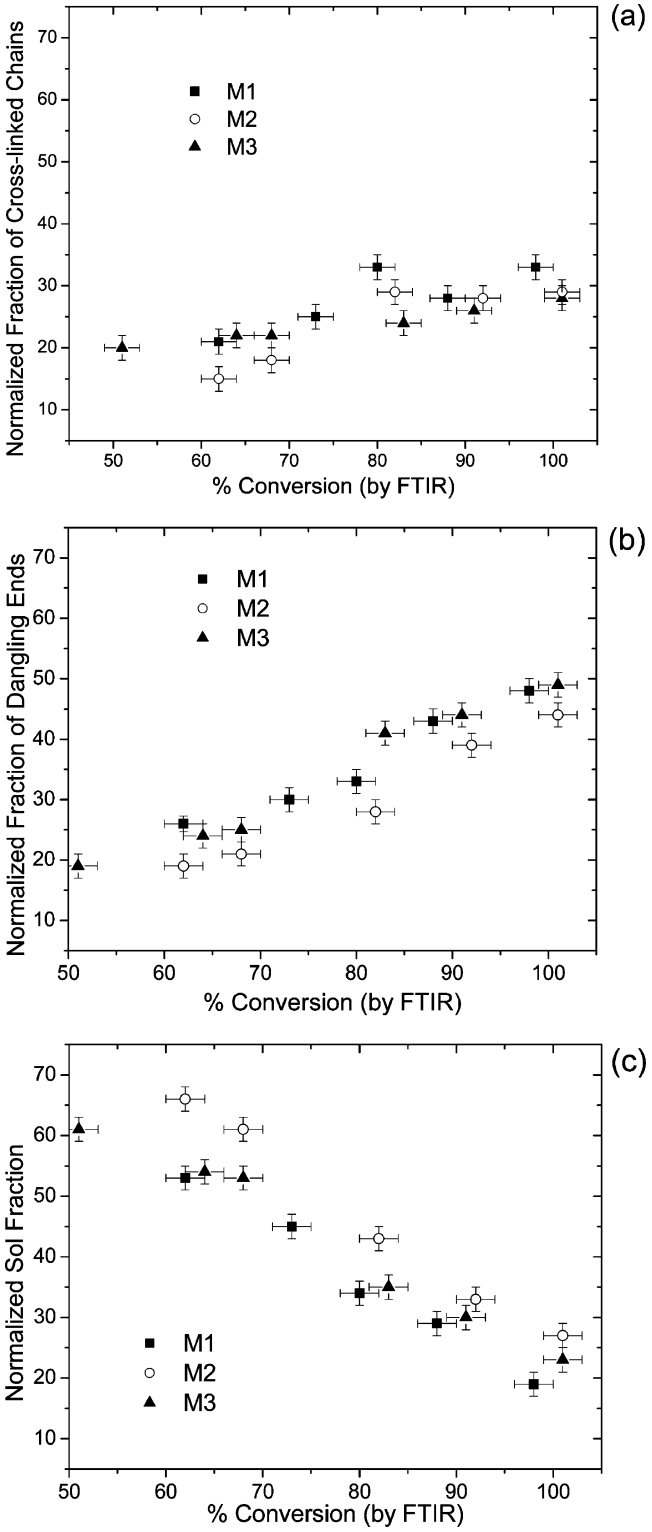

Figure 5. Normalized fractions of network chains in the M-series films possessing different mobilities, as determined from ^{1}H T_2 NMR studies of solvent swollen films: (a) fully cross-linked or low mobility chains, (b) dangling ends or chains with intermediate mobility, and (c) sol or high mobility fraction.

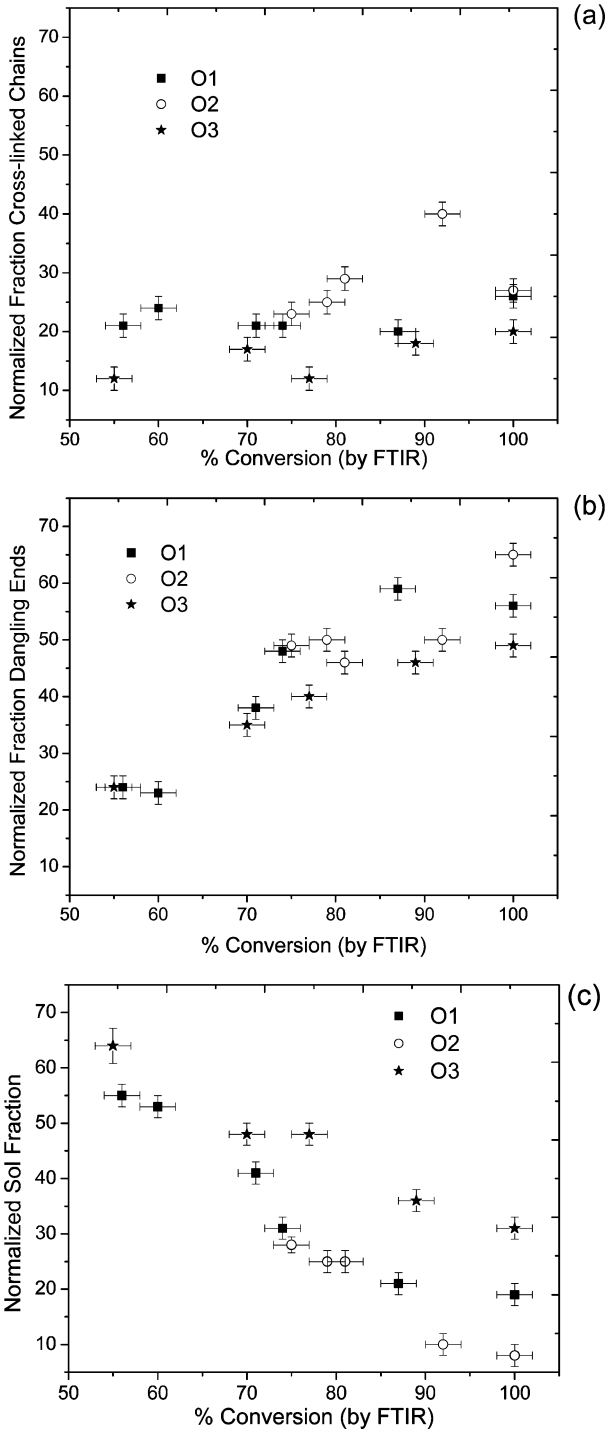

Figure 6. Normalized fractions of network chains in the O series films possessing different mobilities, as determined from ^{1}H T_2 NMR studies of solvent swollen films: (a) fully cross-linked or low mobility chains, (b) dangling ends or chains with intermediate mobility, and (c) sol or high mobility fraction.

overdescriptive and limiting. It may be more appropriate to simply describe populations of low, medium, and high mobility. Each of these contributes to the shape of the ^{1}H T_2 decay curve and allows one to quantitatively treat these types of data. As shown by the solid lines in Figures 4 and 7, the modified Kuhn function describes these data quite well. The fit parameters were obtained for all polymer samples using eq 1. Populations of the low, medium, and high mobility species are plotted for both series of films as a function of degree of conversion in Figures 5−6. The remaining parameters obtained by the fitting procedure are beyond the scope of this discussion but will be the focus of ongoing study.

Without exception, the sol fraction obtained from ^{1}H T_2 NMR data decreases with conversion level of the film. This is consistent with the idea that as the network develops during polymerization, the amount of highly mobile material decreases and eventually reaches a minimum value. For the fully polym-

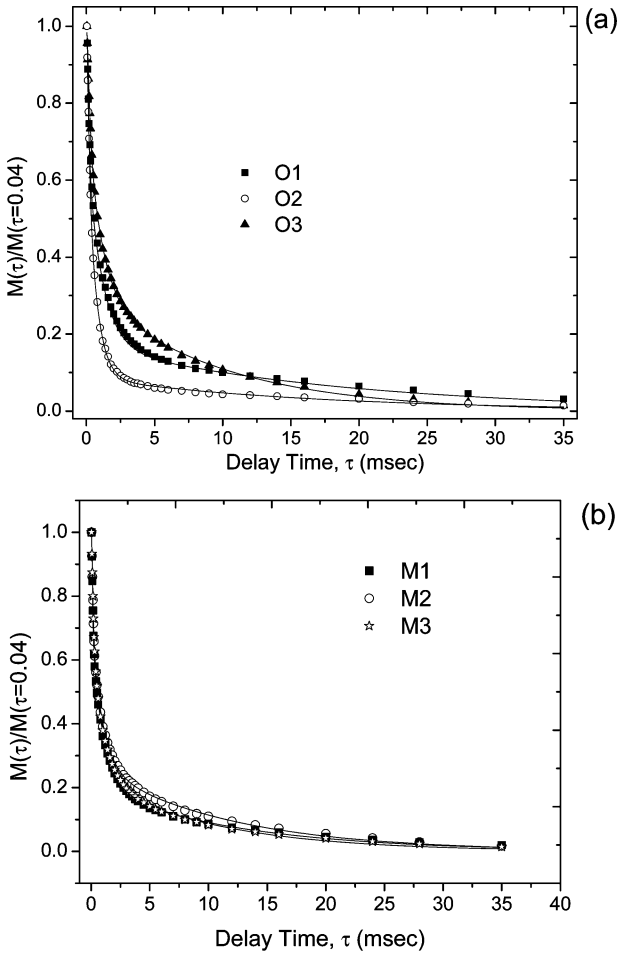

Figure 7. ^{1}H T_2 curves obtained for fully cured solvent swollen M and O series films. Solid lines denote fits to these data.

erized films in these two series, the sol fraction contributes only 10−20% of the polymer. The one exception is the O3 film, which has 31% sol fraction in the 100% polymerized sample, likely due to the highly mobile PPG8000 chain in the 1xPPG8000 oligomer used in this formulation. Even though bound into the network at both ends, a large portion of the polyol component of the oligomer may be quite mobile and appear as a sol-like structure, increasing the apparent amount of sol seen in O3. The other films, each having smaller chain PPG groups, reach a point at which the sol fraction is relatively low.

Similar to the trends in sol fraction, the Kuhn treatment provides some estimate of the amount of fully cross-linked chains and dangling chain ends. In general, the amount of "immobile" network material increases with degree of conversion, as one would have expected. This includes the fraction of cross-linked chains, or network components possessing the least mobility, as well as the dangling chain component, representing material having an intermediate degree of mobility. In general, the rate of increase of the former with degree of conversion is less pronounced than the rate of increase of the latter or of the rate of decrease of sol component.

Comparing the decay curves for the fully polymerized films from each series is also instructive (Figure 7) and demonstrates that the sensitivity of this type of data to conversion level is ultimately tied to the increasing chemical cross-link density of the developing polymer networks. For example, the steepest decay curve in Figure 7 belongs to the O2 film, which has the highest calculated, theoretical cross-link density (2650 g/mol of x-link) in the O series (Table 1). Likewise, the other two O series films have lower cross-link densities (∼8400 g/mol of x-link), and subsequently their ^{1}H T_2 decay curves are relatively less steep. The small difference between the O1 and O3 data in Figure 7a again illustrates the point made previously regarding the flexibility of the oligomer in O3. These data, obtained for films with nearly identical theoretical cross-link densities, should be superimposed if their conversion levels are similar. Since both samples were polymerized to 100% conversion, as determined by FTIR, the slight difference in the curves must originate from some other physical characteristic of these materials. This again suggests that it is likely that the middle of this PPG8000 block in the O3 oligomer has significantly different dynamics than the middle of the PPG2000 chain in the O1 oligomer. In fact, the curves in Figure 7a show that O1 decays slightly faster than O3, especially in the τ range of 2−10 ms, consistent with the relative size and mobility differences of these oligomers.

The relationship of the calculated cross-link density to polymer network properties can also be seen in the values of Young's modulus from stress−strain data for the fully converted polymer network films that is shown in Table 5. For the O series, Young's modulus is expected to reflect the average molecular weight of elastically effective network chains between cross-links, or M_c.[36,37] The values obtained do reflect the calculated cross-link levels given in Table 1, with the modulus values of O1 and O3 being roughly equal and less than the value for O2. This again suggests that the mobility of the large chains in these lightly cross-linked materials, in addition to the cross-link density, is influencing the NMR results.

In a cross-linked network formed from a difunctional oligomer only, M_c would be simply the molecular weight of the oligomer. In the systems studied here, where only one or, in one case, two monofunctional comonomers have been introduced, the visualization of the cross-link density becomes less clear. Because the comonomers introduce the possibility of acrylic chain extension between the oligomer end group cross-link points, it is not clear exactly what constitutes M_c. A number of other defects may also be present in the network as a result of incomplete reaction or various side reactions. Among these are unbound, oligomeric chains of polymerized monomer, dangling chains from either monomer side groups or from partially reacted oligomers, and chain entanglements.[36,37,41] These all will have an impact on measured physical properties.

The NMR decay curves obtained for the fully polymerized M series films (Figure 7b) demonstrate that these measurements are consistent for films having similar theoretical cross-link densities (∼4830 g/mol x-link). The only difference in this series of films is the comonomer used in the formulation, which has no direct effect on cross-linking. Since the oligomer polyol blocks in these formulations are identical (2xPPG2000), there is also no difference in oligomer chain length and hence no expected difference in oligomer chain mobilities. The Young's

Table 5. Properties of Fully Cured Samples

	O1	O2	O3	M1	M2	M3
T_g (°C)[a]	−27	−26	−55 (sh), −37	−33	−44	−40
Young's modulus (MPa)	0.69 ± 0.18	2.47 ± 0.18	0.76 ± 0.06	1.24 ± 0.07	1.15 ± 0.10	1.22 ± 0.05

[a] Determined from the tan δ peak in the DMA curve.

modulus values for all three of the fully polymerized materials in the M series were found to be similar and were between the values measured for the more heavily cross-linked O2 and the more lightly cross-linked O1 and O3 samples.

Also included in Table 5 are the glass transition temperatures for fully polymerized coating networks. These were determined from the maximum of the tan δ curve in dynamic mechanical analysis traces. For the M series, in which the polymerized materials have similar cross-link densities, an analysis based on the Fox equation[42] was applied. If we take the T_g of ethoxylated nonylphenol acrylate homopolymer to be −28 °C,[43] we can use the measured M1 film T_g to calculate the T_g of the 2xPPG2000 oligomer to be approximately −37 °C. Using this value and the measured M2 film T_g, a value of −52 °C is calculated for the Ph8061 homopolymer. Using all three T_g values, a value of −39 °C can then be calculated for M3, which is in good agreement with the measured value of −40 °C. A similar analysis of the O1 and O2 samples would suggest that the 1xPPG2000 oligomer and Ph4003 homopolymer have similar T_g values. However, the differences in cross-link density should also play a role[44,45] even in very lightly cross-linked systems such as these, and this analysis is most likely oversimplified. The O3 sample is the only one that shows clear evidence in the DMA curve of phase separation between a polyol soft block and a diisocyanate/urethane and/or acrylic backbone hard block. This is seen in a distinct low-temperature shoulder at −55 °C on the main tan δ peak at −37 °C. This was also seen in AFM images of the fully polymerized samples (data not shown). These results are consistent with the fact that the separation between hard and soft domains in urethane based systems is expected to become more prevalent as the molecular weight of the polyol component increases.[46]

Conclusions

An integrated approach was taken to the study of polymer coating network development during photopolymerization of a series of fast reacting, low-modulus coating formulations containing urethane/acrylate oligomers and acrylic comonomers. Standard stress−strain measurements on fully cured films showed that the trend in Young's modulus correlates well with the cross-link level based on molecular weight and amount of cross-linking oligomer. Similarly, NMR relaxation studies on fully cured formulations agree with the Young's modulus trend once the high mobility of the oligomer polyol block is accounted for. While stress−strain measurements gave information on the bulk properties of the materials, the NMR relaxation studies reflected the material behavior at a molecular level (specifically all protons in this work). Qualitatively, solid-state NMR ^{1}H T_2 results showed a consistent correlation with cure level for all formulations. In the future, the molecular level of the NMR measurements can be further refined to specific functional groups using cross-polarization experiments (T_{CH}). An additional level of detail could be obtained by studying the incorporation of individual coating components at different stages of the polymerization by analysis of extractables from partially cured samples. Formulation-dependent differences in the rate of comonomer incorporation or in the tendency to form additional, soluble oligomeric materials at intermediate cure levels were seen. A combination of viscosity effects and structure-dependent association of comonomer could account for these observations. The kinetics of network development up to the gel point (∼40% conversion) were also examined by UV rheology and real-time FTIR measurements. It was found that the development of viscoelastic properties did not always increase with increasing monomer conversion rate. In the systems studied here, clear relationships between initial formulation viscosity, acrylate content, conversion rate, and gel time were not obvious. Indeed, the observed conversion rates and gel times seem to be the result of a balance between initial viscosity and acrylate level that is unique for each formulation. Through additional experiments extending the RTIR work to extraction of the propagation and termination rate constants, we hope to further understand the origin of this balance.

Acknowledgment. The authors thank Michael Winningham for helpful discussions.

References and Notes

(1) *Organic Coatings Science and Technology*; Wicks, Z. W., Jr., Jones, F. N., Pappas, S. P., Eds.; John Wiley & Sons: New York, 1992; Vols. 1 and 2.
(2) Decker, C.; Moussa, K. *Makromol. Chem.* **1988**, *189*, 2381−2394.
(3) Decker, C. *J. Polym. Sci., Part A* **1992**, *30*, 913−928.
(4) Jager, W. F.; Lungu, A.; Chen, D. Y.; Neckers, D. C. *Macromolecules* **1997**, *30*, 780−791.
(5) Allen, P. E. M.; Bennett, D. J.; Hagias, S.; Hounslow, A. M.; Ross, G. S.; Simon, G. P.; Williams, D. R. G.; Williams, E. H. *Eur. Polym. J.* **1989**, *25*, 785−789.
(6) Litvinov, V. M.; Dias, A. A. *Macromolecules* **2001**, *34*, 4051−4060.
(7) Hoyle, C. E. In *Radiation Curing: Science and Technology*; Pappas, S. P., Ed.; Plenum: New York, 1992.
(8) Stansbury, J. W.; Dickens, S. H. *Polymer* **2001**, *42*, 6363−6369.
(9) Lee, S. L.; Luciani, A.; Månson, J.-A. E. *Prog. Org. Coat.* **2000**, *38*, 193−197.
(10) Steeman, P. A. M.; Dias, A.; Wienke, D.; Zwartkruis, T. *Macromolecules* **2004**, *37*, 7001−7007.
(11) Fry, C. G.; Lind, A. C. *Macromolecules* **1988**, *21*, 1292−1297.
(12) Litvinov, V. M.; Dias, A. A. *Proc. 50th IWCS* **2001**, 267−272.
(13) Allen, P. E. M.; Simon, G. P.; Williams, D. R. G.; Williams, E. H. *Eur. Polym. J.* **1986**, *22*, 549−557.
(14) Lungu, A.; Neckers, D. C. *Macromolecules* **1995**, *28*, 8147−8152.
(15) Mathias, L. J.; Colletti, R. F. *Macromolecules* **1991**, *24*, 5515−5521.
(16) Peinado, C.; Salvador, E. F.; Alonso, A.; Corrales, T.; Baselga, J.; Catalina, F. *J. Polym. Sci., Part A: Polym. Chem.* **2002**, *40*, 4236−4244.
(17) Peinado, C.; Salvador, E. F.; Corrales, T.; Bosch, P.; Catalina, F. *J. Polym. Sci., Part A: Polym. Chem.* **2004**, *42*, 1227−1238.
(18) Decker, C.; Elzaouk, B.; Decker, D. *Pure Appl. Chem.* **1996**, *A33*, 173−190.
(19) Gasper, S.; Schissel, D.; Baker, L.; Smith, D.; Youngman, R.; Wu, L.; Sonner, S.; Givens, S.; Hancock, R. *Polym. Prepr. (Am. Chem. Soc., Div. Polym. Chem.)* **2003**, *44*, 27−28.
(20) Youngman, R.; Schissel, D.; Gasper, S. *Polym. Prepr. (Am. Chem. Soc., Div. Polym. Chem.)* **2003**, *44*, 350−351.
(21) Swiderski, K. W.; Khudyakov, I. V. *Ind. Chem. Eng. Res.* **2004**, *43*, 6281−6284.
(22) Santhana, P.; Krishnan, G.; Choudhary, V.; Varma, I. K. *J. Macromol. Sci., Rev. Macromol. Chem. Phys.* **1993**, *C33*, 147−180.
(23) McConnell, J. A.; Willard, F. K. *ACS Symp. Ser.* **1990**, *417*, 272−283.
(24) Noren, G. K.; Zimmerman, J. M.; Krajewski, J. J.; Bishop, T. E. *ACS Symp. Ser.* **1990**, *417*, 258−271.
(25) Chambon, F.; Winter, H. H. *Polym. Bull. (Berlin)* **1985**, *13*, 499−504.
(26) Chambon, F.; Winter, H. H. *J. Rheol.* **1987**, *31*, 683−697.
(27) ten Brinke, J. W.; Litvinov, V. M.; Wijnhoven, J. E. G. J.; Noordermeer, J. W. M. *Macromolecules* **2002**, *35*, 10026−10037.
(28) Kuhn, W.; Barth, P.; Hafner, G.; Simon, G.; Schneider, H. *Macromolecules* **1994**, *27*, 5773−5779.
(29) Simon, G.; Baumann, K.; Gronski, W. *Macromolecules* **1992**, *25*, 3624−3628.
(30) Heuert, U.; Knorgen, M.; Menge, H.; Scheler, G.; Schneider, H. *Polym. Bull. (Berlin)* **1996**, *37*, 489−496.
(31) Knorgen, M.; Menge, H.; Hempel, G.; Schneider, H.; Ries, M. E. *Polymer* **2002**, *43*, 4091−4096.
(32) Steren, C. A.; Monti, G. A.; Marzocca, A. J.; Cerveny, S. *Macromolecules* **2004**, *37*, 5624−5629.
(33) Menge, H.; Hotopf, S.; Heuert, U.; Schneider, H. *Polymer* **2000**, *41*, 3019−3027.
(34) Litvinov, V. M.; Steeman, P. A. M. *Macromolecules* **1999**, *32*, 8476−8490.
(35) Saalwachter, K. *Macromolecules* **2005**, *38*, 1508−1512.
(36) Kloosterboer, J. *Adv. Polym. Sci.* **1984**, *84*, 1−61.

(37) Dušek, K.; Dušková-Smrčková, M. *Prog. Polym. Sci.* **2000**, *25*, 1215−1260.
(38) Lovell, L. G.; Stansbury, J. W.; Syrpes, D. C.; Bowman, C. N. *Macromolecules* **1999**, *32*, 3913−3921.
(39) Jansen, J. F. G. A.; Dias, A. A.; Dorschu, M.; Coussens, B. *Macromolecules* **2003**, *36*, 3861−3873.
(40) Borgia, G. C.; Fantazzini, A.; Ferrando, A.; Maddinelli, G. *Magn. Reson. Imaging* **2001**, *19*, 405−409.
(41) *Thermosetting Polymers*; Pascault, J.-P., Sautereau, H., Verdu, J., Williams, R. J. J., Eds.; Marcel Dekker: New York, 2002.
(42) Fox, T. G.; Loshaek, S. *J. Polym. Sci.* **1955**, *15*, 371−390.
(43) Sartomer Application Bulletin 4013.
(44) Stutz, H.; Illers, K.-H.; Mertes, J. *J. Polym. Sci., Part B* **1990**, *28*, 1483−1498.
(45) Nabeth, B.; Corniglion, I.; Pascault, J. P. *J. Polym. Sci., Part B* **1996**, *34*, 401−417.
(46) Barbeau, Ph.; Gerard, J. F.; Magny, B.; Pascault, J. P.; Vigier, G. *J. Polym. Sci., Part B* **1999**, *37*, 919−937.

MA051918J